

Channel State Tracking for Large-Scale Distributed MIMO Communication Systems

D. Richard Brown, III, *Senior Member, IEEE*, Rui Wang, *Student Member, IEEE*, and Soura Dasgupta, *Fellow, IEEE*

Abstract—This paper considers the problem of estimating and tracking channels in a distributed transmission system with N_t transmit nodes and N_r receive nodes. Since each node in the distributed transmission system has an independent local oscillator, the effective channel between each transmit node and each receive node has time-varying phase and frequency offsets which must be tracked and predicted to facilitate coherent transmission. A linear time-invariant state-space model is developed and is shown to be observable but nonstabilizable. To quantify the steady-state performance of a Kalman filter channel tracker, two methods are developed to efficiently compute the steady-state prediction covariance. The first method requires the solution of a $2(N_t + N_r - 1)$ -dimensional discrete-time algebraic Riccati equation, but allows for nonhomogenous oscillator parameters. The second method requires the solution of four two-dimensional discrete-time algebraic Riccati equations but requires homogenous oscillator parameters for all nodes in the system. An asymptotic analysis is also presented for the homogenous oscillator case for systems with a large number of transmit and receive nodes with closed-form results for all of the elements in the asymptotic prediction covariance as a function of the carrier frequency, oscillator parameters, and channel measurement period. Numeric results confirm the analysis and demonstrate the effect of the oscillator parameters on the ability of the distributed transmission system to achieve coherent transmission.

Index Terms—Asymptotic analysis, channel prediction, coherent transmission, discrete-time algebraic Riccati equation, distributed communication systems, oscillator dynamics.

I. INTRODUCTION

WE consider the distributed multi-input multi-output (MIMO) communication scenario in Fig. 1 where a transmit cluster with N_t transmit nodes communicates with a receive cluster with N_r receive nodes. The transmit cluster is assumed to use coherent transmission techniques, e.g., distributed beamforming [1], distributed nullforming [2], and/or distributed zero-forcing beamforming [3]. It is well known that coherent transmission techniques require channel state information at the transmitters (CSIT). Several techniques have been

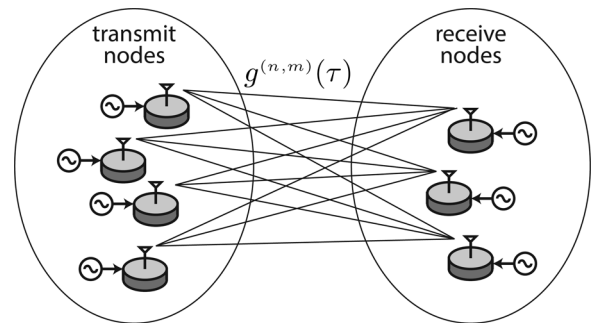


Fig. 1. Distributed MIMO system model with N_t transmit nodes and N_r receive nodes. Each node possesses a single antenna and an independent oscillator.

proposed to address this issue for distributed MIMO systems, with the goal of providing CSIT either implicitly or explicitly. These include receiver-coordinated explicit feedback [2], [4]–[9], receiver-coordinated summarized feedback [10]–[12], master-slave synchronization with retrodirective transmission [1], round-trip retrodirective transmission [13]–[15], and two-way synchronization with retrodirective transmission [16], [17]. Each of these techniques has advantages and disadvantages in particular applications, as discussed in the survey article [18].

In this paper, we focus on the receiver-coordinated explicit feedback scenario in which the receive cluster measures the channels and provides explicit feedback to the transmit cluster to facilitate coherent transmission. This approach can be used in time-division-duplex (TDD) and frequency-division-duplex (FDD) systems. We assume no external source of synchronization in the system, hence the time-varying phase and frequency offsets in each effective channel (which includes propagation as well as oscillator offsets) must be tracked and predicted to facilitate coherent transmission. We consider a scenario in which the effective channels are tracked by one or more Kalman filters.

Kalman filters have been used extensively in clock tracking and synchronization, e.g., [19]–[22], including global positioning systems (GPS) [23], the network time protocol (NTP) [24], and the precision time protocol (PTP) [25]. The focus of this prior work, however, is on tracking and correcting clock offsets between a single pair of nodes (typically a master node such as a satellite and a slave node such as a GPS receiver). The distributed MIMO setting of Fig. 1 generalizes this idea to tracking a matrix of clock offsets corresponding to the collection of effective channels between all of the transmitters and receivers. Since the dynamics of these channels are correlated, tracking channels individually is suboptimum.

Manuscript received June 10, 2014; revised November 24, 2014; accepted February 10, 2015. Date of publication February 26, 2015; date of current version April 13, 2015. The associate editor coordinating the review of this manuscript and approving it for publication was Prof. Trac Tran. This work was supported by the National Science Foundation awards CCF-1302104 and CCF-1319458. Portions of this paper were presented at the Conference on Information Sciences and Systems (CISS), Princeton, NJ, USA, March 2014.

D. R. Brown, III, and R. Wang are with the Department of Electrical and Computer Engineering, Worcester Polytechnic Institute, Worcester, MA 01609 USA (e-mail: drb@wpi.edu; rwang@wpi.edu).

S. Dasgupta is with the Department of Electrical and Computer Engineering, University of Iowa, Iowa City IA 52242 USA (e-mail: dasgupta@engineering.uiowa.edu).

Digital Object Identifier 10.1109/TSP.2015.2407316

A few recent papers have analyzed the performance of distributed beamforming and distributed nullforming in the distributed MIMO setting [6]–[9] and have shown that the performance of these coherent transmission techniques can be expressed as simple functions of the channel phase prediction variance [26]. The early papers in this area made the simplifying assumption that each channel was tracked individually or each receiver tracked only its own N_t channels. While the latter approach is an improvement on tracking channels individually, it does not exploit correlations across receivers. More recently, the idea of “unified” tracking has been studied in which all of $N_t N_r$ channels in the system are jointly tracked [9]. A system with unified tracking achieves optimal performance by exploiting the correlations across all of the effective channels. As verified in the numerical results of Section VI and elaborated upon in Section III-C, unified tracking can significantly outperform approaches which separately track each effective channel.

The main contribution of this paper is a formal analysis of the stability and steady-state behavior of a Kalman filter tracker for the effective channel states of an unsynchronized distributed MIMO communication system in the case where the magnitudes of the propagation channels $|g^{(n,m)}(\tau)|$ are separately tracked and are slowly-varying. In particular, although the state-space model for the effective channel states developed in Section II is completely observable but not stabilizable, we show that the Kalman filter is asymptotically stable subject to a properly chosen initial prediction covariance. We then analyze the steady-state prediction covariance of the Kalman filter tracker, establishing existence and uniqueness of a particular positive semidefinite “strong” solution, and develop two methods to efficiently solve the resulting discrete-time algebraic Riccati equation (DARE) for this strong solution. The first method uses a similarity transformation to cast the system in a controllable staircase form and reduces the original $2N_t N_r$ -dimensional DARE to a $2(N_t + N_r - 1)$ -dimensional DARE. This method is also general in that it allows for non-homogeneous oscillator and measurement noise parameters. The second method exploits the particular structure of the state-space model and uses a similarity transform to cast the system in a block diagonal form. When the oscillator parameters and measurement noise variance are homogenous across all nodes in the system, this method reduces to simply solving four 2-dimensional DAREs. This second method is particularly useful for large-scale systems, e.g., distributed massive MIMO systems [27], [28], since the dimension of the DAREs is not a function of the transmit or receive cluster sizes. To fully characterize the behavior of the prediction covariance for large systems, we present an asymptotic analysis for the case when $N_t \rightarrow \infty$ and $N_r = \eta N_t$, and develop closed-form results for all of the elements in the asymptotic prediction covariance as a function of the carrier frequency, oscillator parameters, and channel measurement period. Numeric results confirm the analysis and demonstrate the effect of the oscillator parameters on the ability of the distributed transmission system to achieve coherent transmission.

The rest of the paper is organized as follows. We first develop the system model, local oscillator model, and the unified state space model for tracking all of the effective channels in the system in Section II. We then discuss the optimal

channel tracker in Section III and establish its asymptotic stability. The steady-state prediction covariance is analyzed in Section IV where two reduced-dimensional methods are developed to facilitate efficient calculation of the positive semidefinite steady-state prediction covariance matrix. An asymptotic analysis of the steady-state prediction covariance is presented in Section V. Numerical results are given in Section VI, followed by conclusions in Section VII. Proofs of the main theorems are provided in the Appendices.

Notation: The $n \times n$ identity matrix is denoted \mathbf{I}_n and $\mathbf{1}_n$ denotes a length n vector of all ones. We use $\mathbb{E}\{\cdot\}$, $(\cdot)^\top$, and $(\cdot)^{-\top}$ for expectation, transposition, and inverse transposition, respectively. We use \otimes to denote the Kronecker product. For any matrices \mathbf{A} and \mathbf{B} with the same dimension and integer $n \geq 1$, we define

$$\begin{aligned} \Gamma_n(\mathbf{A}, \mathbf{B}) &:= \mathbf{I}_n \otimes \mathbf{A} + \mathbf{1}_n \mathbf{1}_n^\top \otimes \mathbf{B} \\ &= \begin{bmatrix} \mathbf{A} + \mathbf{B} & \mathbf{B} & \cdots & \mathbf{B} \\ \mathbf{B} & \mathbf{A} + \mathbf{B} & & \\ \vdots & & \ddots & \\ \mathbf{B} & & & \mathbf{A} + \mathbf{B} \end{bmatrix}. \end{aligned} \quad (1)$$

II. SYSTEM MODEL

Each node in the system shown in Fig. 1 is assumed to possess a single antenna. The nodes in the system are not assumed to be synchronized. The nominal transmit frequency in the forward link from the distributed transmit cluster to the receivers is at ω_c . All forward link channels are modeled as narrowband and linear. We denote the channel from transmit node n to receive node m at carrier frequency ω_c as $g^{(n,m)}(\tau) \in \mathbb{C}$ for transmit node $n = 1, \dots, N_t$ and receive node $m = 1, \dots, N_r$. These propagation channels, in contrast to the time-varying “effective” channels described below, do not include the effect of carrier phase and/or frequency offsets between transmit node n and receive node m .

Fig. 2 shows the *effective* narrowband channel model from transmit node n to receive node m including the effects of propagation and carrier offset. Transmissions $n \rightarrow m$ are conveyed on a carrier nominally at ω_c generated at transmit node n , incur a phase shift of $\psi^{(n,m)}(\tau) = \angle g^{(n,m)}(\tau)$ over the wireless channel, and are then downmixed by receive node m using its local carrier nominally at ω_c . At time τ , the effective narrowband channel from transmit node n to receive node m is modeled as

$$\begin{aligned} h^{(n,m)}(\tau) &= g^{(n,m)}(\tau) e^{j(\phi_t^{(n)}(\tau) - \phi_r^{(m)}(\tau))} \\ &= |g^{(n,m)}(\tau)| e^{j\phi^{(n,m)}(\tau)} \end{aligned} \quad (2)$$

where $\phi_t^{(n)}(\tau)$ and $\phi_r^{(m)}(\tau)$ are the local carrier phase offsets at transmit node n and receive node m , respectively, at time τ with respect to an ideal carrier reference, and

$$\phi^{(n,m)}(\tau) := \phi_t^{(n)}(\tau) + \psi^{(n,m)}(\tau) - \phi_r^{(m)}(\tau)$$

is the pairwise phase offset after propagation between transmit node n and receive node m at time τ .

We consider an approach in which the effective channels are measured at the receive nodes and feedback is provided by the receive nodes to the transmit nodes to facilitate coherent

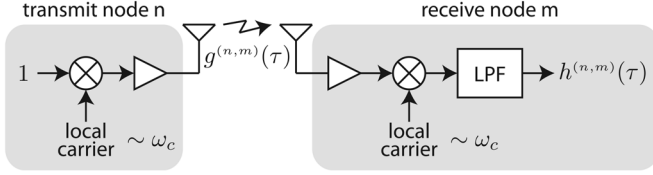


Fig. 2. Effective narrowband channel model including the effects of propagation, transmit and receive gains, and carrier offset.

transmission. Note that there are two sources of independent dynamics in each effective channel: (i) propagation dynamics and (ii) oscillator dynamics. Since the oscillator dynamics do not affect the channel magnitudes, we assume that the channel magnitudes $|g^{(n,m)}(\tau)|$ are tracked separately using methods as in [29] and are slowly-varying such that they are known perfectly. The problem of estimating and tracking the effective channels $h^{(n,m)}(\tau)$ then reduces to estimating and tracking the pairwise phase offsets $\phi^{(n,m)}(\tau)$. The following sections provide an overview of basic oscillator dynamics and then develop a unified dynamic model for the phase and frequency offsets of the effective channels.

A. Oscillator Dynamics

Each local oscillator in the system has inherent frequency and phase offsets with respect to some nominal reference and also behaves stochastically, causing phase offset variations in each effective channel from transmit node n to receive node m even when the propagation channels $g^{(n,m)}$ are otherwise time invariant. This section describes a discrete-time dynamic model for the local oscillator dynamics at each transmit and receive node.

Based on the two-state oscillator models in [30], [31], we define the discrete-time state of the n^{th} transmit node's carrier as

$$\mathbf{x}_t^{(n)}[k] := \begin{bmatrix} \phi_t^{(n)}[k] \\ \omega_t^{(n)}[k] \end{bmatrix}$$

where $\phi_t^{(n)}[k] = \phi_t^{(n)}(kT_0)$ and $\omega_t^{(n)}[k] = \omega_t^{(n)}(kT_0)$ correspond to the carrier phase offset in radians and frequency offset in radians per second, respectively, at transmit node n with respect to an ideal carrier phase reference and where $T_0 > 0$ is the state update period. The state update of the n^{th} transmit node's carrier follows

$$\mathbf{x}_t^{(n)}[k+1] = \mathbf{f}\mathbf{x}_t^{(n)}[k] + \mathbf{u}_t^{(n)}[k] \quad (3)$$

with

$$\mathbf{f} := \begin{bmatrix} 1 & T_0 \\ 0 & 1 \end{bmatrix}. \quad (4)$$

The local process noise vector $\mathbf{u}_t^{(n)}[k] \stackrel{\text{i.i.d.}}{\sim} \mathcal{N}(0, \mathbf{Q}_t^{(n)})$ causes the carrier derived from the local oscillator at transmit node n to deviate from an ideal affine phase trajectory. The covariance of the discrete-time process noise is derived from a continuous-time model in [30] and can be written as

$$\mathbf{Q}_t^{(n)} = \omega_c^2 T_0 \begin{bmatrix} \alpha_t^{(n)} + \beta_t^{(n)} \frac{T_0^2}{3} & \beta_t^{(n)} \frac{T_0}{2} \\ \beta_t^{(n)} \frac{T_0}{2} & \beta_t^{(n)} \end{bmatrix} \quad (5)$$

where ω_c is the nominal common carrier frequency in radians per second and $\alpha_t^{(n)}$ (units of seconds) and $\beta_t^{(n)}$ (units of Hertz)

are the process noise parameters corresponding to white frequency noise and random walk frequency noise, respectively. The process noise parameters $\alpha_t^{(n)}$ and $\beta_t^{(n)}$ can be estimated by fitting the theoretical Allan variance $\sigma_y^2(\tau) = \frac{\alpha_t^{(n)}}{\tau} + \frac{\beta_t^{(n)}\tau}{3}$ to experimental measurements of the Allan variance over a range of τ values. For example, a least squares fit to the Allan variance specifications for a Rakon RPFO45 oven-controlled oscillator [32] yields $\alpha_t^{(n)} = 2.31 \times 10^{-21}$ and $\beta_t^{(n)} = 6.80 \times 10^{-23}$. Typical Allan variance values for various types of oscillators are tabulated in [33].

The receive nodes in the system also have independent local oscillators used to generate carriers for downmixing that are governed by the same dynamics as (3) with state $\mathbf{x}_r^{(m)}[k]$, process noise $\mathbf{u}_r^{(m)}[k] \stackrel{\text{i.i.d.}}{\sim} \mathcal{N}(0, \mathbf{Q}_r^{(m)})$, and process noise parameters $\alpha_r^{(m)}$ and $\beta_r^{(m)}$ as in (5) for $m = 1, \dots, N_r$.

B. Pairwise Offset States and Observations

To facilitate coherent transmission, the receivers in the system periodically measure the effective channels from the transmit cluster and feed back their measurements to facilitate channel tracking at the transmitters as in [2], [6]–[9]. Since the receive nodes can only observe the relative phase and frequency of the transmit nodes after propagation, we define the *pairwise offset* after propagation as

$$\boldsymbol{\delta}^{(n,m)}[k] := \begin{bmatrix} \phi^{(n,m)}[k] \\ \omega^{(n,m)}[k] \end{bmatrix} = \mathbf{x}_t^{(n)}[k] + \begin{bmatrix} \psi^{(n,m)} \\ 0 \end{bmatrix} - \mathbf{x}_r^{(m)}[k]$$

where $\psi^{(n,m)}$ is the propagation phase¹. Note that $\boldsymbol{\delta}^{(n,m)}[k]$ is governed by the state update

$$\boldsymbol{\delta}^{(n,m)}[k+1] = \mathbf{f}\boldsymbol{\delta}^{(n,m)}[k] + \mathbf{u}_t^{(n)}[k] - \mathbf{u}_r^{(m)}[k]. \quad (6)$$

We assume that observations are so short as to only provide useful phase estimates. An observation of the $n \rightarrow m$ channel at receive node m is then modeled as

$$y^{(n,m)}[k] = \mathbf{h}\boldsymbol{\delta}^{(n,m)}[k] + v^{(n,m)}[k]$$

where

$$\mathbf{h} := [1 \quad 0] \quad (7)$$

and $v^{(n,m)}[k] \stackrel{\text{i.i.d.}}{\sim} \mathcal{N}(0, r)$ is scalar measurement noise with variance r assumed to be spatially and temporally i.i.d., and independent of the process noise. The measurement noise variance r depends on the several factors including the signal-to-noise ratio of the channel and the duration of the measurement signal. Bounds on the measurement noise variance for maximum likelihood phase estimators are given in [34].

The use of a pairwise offset state is important in our tracking scenario since it provides states which are physically meaningful as well as observable. It is straightforward to confirm the observability of $[\mathbf{f}, \mathbf{h}]$ as defined in (4) and (7) for any $T_0 > 0$. The following section develops a unified dynamic model comprising all of the pairwise offset states in the system.

¹For clarity of exposition and consistent with previous assumptions, the propagation phase is assumed here to be slowly-varying with respect to the oscillator dynamics. If the propagation phase $\psi^{(n,m)}[k]$ is not slowly varying, its dynamics can also be incorporated in the pairwise offset state $\boldsymbol{\delta}^{(n,m)}[k]$.

We prove that this unified model is also completely observable in Section II-D.

C. Unified Dynamic Model

While it is possible to track each of the pairwise offset states $\delta^{(n,m)}[k]$ in (6) individually, it is straightforward to see that the pairwise offset states do not have independent dynamics. For example, $\delta^{(1,2)}[k]$ and $\delta^{(1,3)}[k]$ are correlated since they share a common process noise term $\mathbf{u}_t^{(1)}[k]$. This section develops a *unified* dynamic model for all of the pairwise offsets in the system to facilitate optimal unified tracking. As shown in [9] in a zero-forcing distributed beamforming scenario, unified tracking can provide significant gains in the depth of the nulls with respect to individual channel tracking.

We define the vector of unified pairwise offsets as

$$\delta[k] := \begin{bmatrix} \delta^{(1)}[k] \\ \vdots \\ \delta^{(N_r)}[k] \end{bmatrix} \in \mathbb{R}^{2N_t N_r}$$

with

$$\delta^{(m)}[k] := \begin{bmatrix} \delta^{(1,m)}[k] \\ \vdots \\ \delta^{(N_t,m)}[k] \end{bmatrix} \in \mathbb{R}^{2N_t}$$

From (6), the unified state dynamics follow as

$$\begin{aligned} \delta[k+1] &= \begin{bmatrix} \mathbf{f} & & \\ & \ddots & \\ & & \mathbf{f} \end{bmatrix} \delta[k] + \begin{bmatrix} \mathbf{u}_t^{(1)}[k] - \mathbf{u}_r^{(1)}[k] \\ \vdots \\ \mathbf{u}_t^{(N_t)}[k] - \mathbf{u}_r^{(N_r)}[k] \end{bmatrix} \\ &= \mathbf{F}\delta[k] + \mathbf{G}\mathbf{u}[k] \end{aligned} \quad (8)$$

with \mathbf{f} defined in (4), the process noise vector

$$\mathbf{u}[k] := \begin{bmatrix} \mathbf{u}_t^{(1)}[k] \\ \vdots \\ \mathbf{u}_t^{(N_t)}[k] \\ \mathbf{u}_r^{(1)}[k] \\ \vdots \\ \mathbf{u}_r^{(N_r)}[k] \end{bmatrix} \in \mathbb{R}^{2(N_t+N_r)}$$

with $\mathbf{u}[k] \stackrel{\text{i.i.d.}}{\sim} \mathcal{N}(0, \mathbf{U})$, covariance matrix $\mathbf{U} = \mathbb{E}[\mathbf{u}[k]\mathbf{u}^\top[k]] = \text{blockdiag}(\mathbf{Q}_t^{(1)}, \dots, \mathbf{Q}_t^{(N_t)}, \mathbf{Q}_r^{(1)}, \dots, \mathbf{Q}_r^{(N_r)})$, and

$$\mathbf{G} := \begin{bmatrix} \mathbf{I}_{2N_t} & \mathbf{J}_{2N_t} & & \\ \vdots & & \ddots & \\ \mathbf{I}_{2N_t} & & & \mathbf{J}_{2N_t} \end{bmatrix} \in \mathbb{R}^{2N_t N_r \times 2(N_t+N_r)} \quad (9)$$

where $\mathbf{J}_{2N_t} := -[\mathbf{I}_2, \dots, \mathbf{I}_2]^\top \in \mathbb{R}^{2N_t \times 2}$. The $N_t N_r$ -dimensional vector observation is then

$$\begin{aligned} \mathbf{y}[k] &= \begin{bmatrix} \mathbf{h} & & \\ & \ddots & \\ & & \mathbf{h} \end{bmatrix} \delta[k] + \mathbf{v}[k] \\ &= \mathbf{H}\delta[k] + \mathbf{v}[k] \end{aligned} \quad (10)$$

with \mathbf{h} defined in (7), $\mathbf{H} \in \mathbb{R}^{N_t N_r \times 2N_t N_r}$, and

$$\mathbf{v}[k] := \begin{bmatrix} v^{(1,1)}[k] \\ \vdots \\ v^{(N_t, N_r)}[k] \end{bmatrix} \in \mathbb{R}^{N_t N_r}$$

denoting the i.i.d. measurement noise with $\mathbf{v}[k] \stackrel{\text{i.i.d.}}{\sim} \mathcal{N}(0, \mathbf{R})$ and $\mathbf{R} = r\mathbf{I}_{N_t N_r}$.

D. Model Properties

This section analyzes qualitative properties of the state variable realization (SVR) specified in (8) and (10) as these properties are critical to the behavior and performance of state tracking as well as the existence and uniqueness of steady-state prediction covariances as analyzed in Section IV.

Two key properties in analyzing the behavior of the steady state Kalman Filter are controllability and stabilizability. We first define the notion of complete controllability below.

Definition 1: A discrete-time system is completely controllable if, given an arbitrary destination point in the state space, there is an input sequence that will bring the system from any initial state to this point in a finite number of steps [35].

The concept of stabilizability is closely related to controllability. Recall that an unstable mode of a linear time-invariant discrete-time system is an eigenvector associated with an eigenvalue of the state transition matrix \mathbf{F} with magnitude greater than or equal to one. Stabilizability is defined below.

Definition 2: A system is stabilizable if all its unstable modes are controllable [36].

Since all modes of the SVR specified in (8) and (10) are unstable, such an SVR is stabilizable if and only if it is completely controllable.

Denote $\mathbf{U} = \mathbb{E}[\mathbf{u}[k]\mathbf{u}^\top[k]]$ and the Cholesky factorization of \mathbf{U} as $\mathbf{U}^{1/2}$ such that $\mathbf{U}^{1/2}(\mathbf{U}^{1/2})^\top = \mathbf{U}$. A common test for complete controllability [35] is to compute the rank of the ‘‘controllability matrix’’ of the pair $[\mathbf{F}, \mathbf{G}\mathbf{U}^{1/2}]$, i.e.,

$$\mathcal{C} = [\mathbf{G}\mathbf{U}^{1/2} \quad \mathbf{F}\mathbf{G}\mathbf{U}^{1/2} \quad \dots \quad \mathbf{F}^{2N_t N_r - 1} \mathbf{G}\mathbf{U}^{1/2}] \quad (11)$$

where $\mathcal{C} \in \mathbb{R}^{2N_t N_r \times (2N_t N_r + 2(N_t + N_r))}$. The SVR specified in (8) and (10) is completely controllable if and only if $\text{rank}(\mathcal{C}) = 2N_t N_r$.

It can be shown that the rank of $\mathbf{G}\mathbf{U}^{1/2}$ is $2(N_t + N_r - 1)$. Intuitively, this is a consequence of the fact that, while the number of states in the unified dynamic model grows according to the product $N_t N_r$, the number of independent oscillators grows according to the sum $N_t + N_r$. In fact $2(N_t N_r - N_t - N_r + 1)$ state elements can be determined from $2(N_t + N_r - 1)$ state elements, to up to unknown, but deterministic, bias terms, representing differences of the channel phases $\psi^{(n,m)}$. This causes the process noise $\mathbf{G}\mathbf{u}[k]$ to span only a subspace of the $2N_t N_r$ -dimensional state space. Hence, $\text{rank}(\mathcal{C}) \leq 2(N_t + N_r - 1) \leq 2N_t N_r$ where the second inequality is strict if $N_t > 1$ and $N_r > 1$. In other words, the SVR specified in (8) and (10) is not stabilizable unless $N_t = 1$ or $N_r = 1$. As discussed in Section III, this lack of stabilizability results in additional conditions that must be satisfied for a Kalman filter tracker to be asymptotically stable.

We now consider the observability of the SVR specified in (8) and (10).

Definition 3: A system is completely observable if its initial state can be fully and uniquely recovered from a finite number of observations of its output (in the absence of noise) and knowledge of its input [35].

A common test to check complete observability for linear time-invariant systems is to compute the rank of the “observability matrix” of the pair $[\mathbf{F}, \mathbf{H}]$, given as

$$\mathcal{O} = \begin{bmatrix} \mathbf{H} \\ \mathbf{HF} \\ \vdots \\ \mathbf{HF}^{2N_t N_r - 1} \end{bmatrix} \quad (12)$$

where $\mathcal{O} \in \mathbb{R}^{(N_t N_r (2N_t N_r)) \times 2N_t N_r}$. The system is completely observable if and only if $\text{rank}(\mathcal{O}) = 2N_t N_r$. The following lemma establishes that the SVR specified in (8) and (10) is completely observable, an important property that will be used in several later results.

Lemma 1: Given $T_0 > 0$, $[\mathbf{H}, \mathbf{F}]$ as specified in (8) and (10) is completely observable.

Proof: Observe that $\mathbf{H} = \mathbf{I}_{N_r N_t} \otimes \mathbf{h}$ and $\mathbf{F}^k = \mathbf{I}_{N_r N_t} \otimes \mathbf{f}^k$ with

$$\mathbf{f}^k = \begin{bmatrix} 1 & kT_0 \\ 0 & 1 \end{bmatrix}.$$

Since $\mathbf{h}\mathbf{f}^k = [1, kT_0]$, we can write

$$\mathbf{HF}^k = \mathbf{I}_{N_r N_t} \otimes \mathbf{h}\mathbf{f}^k \in \mathbb{R}^{N_t N_r \times 2N_t N_r}.$$

It is straightforward to see that the observability matrix in (12) has row rank $2N_t N_r$ for any $T_0 > 0$ since the square matrix

$$\mathcal{O}' = \begin{bmatrix} \mathbf{H} \\ \mathbf{HF} \end{bmatrix} \in \mathbb{R}^{2N_t N_r \times 2N_t N_r}$$

is full rank when $T_0 > 0$. Hence $[\mathbf{H}, \mathbf{F}]$ as specified in (8) and (10) is completely observable. ■

A condition necessary for the Kalman Filter to converge to a well-defined steady-state solution is that the SVR in (8) and (10) is detectable. We conclude this section by defining detectability below.

Definition 4: A system is detectable if all its unstable modes are observable [36].

Since complete observability suffices for detectability, the SVR specified in (8) and (10) is indeed detectable.

III. OPTIMAL CHANNEL ESTIMATION AND TRACKING

It is straightforward to see that the dynamic model and observations specified in (8) and (10) comprise a standard linear time-invariant (LTI) Gauss-Markov model with zero-mean temporally i.i.d. Gaussian mutually independent process and measurement noises with process noise covariance \mathbf{Q} and measurement noise covariance \mathbf{R} . Further assuming an independent Gaussian initial state $\boldsymbol{\delta}[0]$, it follows that a standard Kalman filter [36] can be used to generate optimal (both minimum variance and maximum likelihood) estimates and one-step predictions of the unified pairwise offset state $\boldsymbol{\delta}[k]$.

A. Asymptotic Stability of the Kalman Filter

We denote $\hat{\boldsymbol{\delta}}[k|\ell]$ as the MMSE estimate of the state $\boldsymbol{\delta}[k]$ given observations $\{y[0], \dots, y[\ell]\}$ and $\tilde{\boldsymbol{\delta}}[k|\ell] = \hat{\boldsymbol{\delta}}[k|\ell] - \boldsymbol{\delta}[k]$ as the estimation error. As part of the Kalman filter recursion, the (one-step) prediction covariance at time k , defined as

$$\mathbf{P}[k] := \mathbb{E} \left\{ \tilde{\boldsymbol{\delta}}[k|k-1] (\tilde{\boldsymbol{\delta}}[k|k-1])^\top \right\} \in \mathbb{R}^{2N_t N_r \times 2N_t N_r}$$

is updated via the Riccati difference equation

$$\mathbf{P}[k+1] = \mathbf{F}\mathbf{P}[k]\mathbf{F}^\top - \mathbf{F}\mathbf{P}[k]\mathbf{H}^\top (\mathbf{H}\mathbf{P}[k]\mathbf{H}^\top + \mathbf{R})^{-1} \mathbf{H}\mathbf{P}[k]\mathbf{F}^\top + \mathbf{Q} \quad (13)$$

given an initial prediction covariance $\mathbf{P}[0]$.

Although the system specified in (8) and (10) is not stabilizable, the following theorem (adapted from [37, Theorem 4.1]) establishes conditions sufficient for the Kalman filter to be asymptotically stable.

Theorem 1: If \mathbf{F} , \mathbf{F}^{-1} , \mathbf{Q} , and \mathbf{R}^{-1} are all bounded, $[\mathbf{H}\mathbf{R}^{-1/2}, \mathbf{F}]$ is completely observable, and

$$\mathbf{W}[k] = \mathbf{F}^k \mathbf{P}[0] (\mathbf{F}^k)^\top + \sum_{\ell=1}^k \mathbf{F}^{k-\ell} \mathbf{Q} (\mathbf{F}^{k-\ell})^\top$$

is nonsingular for some k where $\mathbf{P}[0]$ is the initial prediction covariance, then the Kalman filter is asymptotically stable.

The boundedness conditions are satisfied for the system specified in (8) and (10) under the usual assumptions that $r > 0$, $T_0 < \infty$, and the oscillator parameters are finite. Lemma 1 establishes complete observability. The final condition, $\mathbf{W}[k]$ is non-singular for some k , can be thought of as an interaction between the initial prediction covariance $\mathbf{P}[0]$ and the controllability Gramian. The singularity of the summation in the expression for $\mathbf{W}[k]$ represents a lack of reachability of $[\mathbf{F}, \mathbf{Q}^{1/2}]$. Suppose $\mathbf{W}[k]$ is singular for all k and consider its nontrivial null space. Then this null space represents a linear combination of states that are perfectly known at $k = 0$, and are not affected by the process noise. Thus the Kalman filter does not update these modes. Should they be on or outside the unit circle, then the resulting filter cannot be stable. Observe that it is sufficient (but not necessary) to select $\mathbf{P}[0]$ to be any positive definite matrix to satisfy the condition given in the theorem for the system specified in (8) and (10).

The prediction covariance is particularly important for distributed coherent transmission systems since the achievable performance of distributed beamforming and nullforming is a direct function of the phase prediction variance [9], [26]. The phase prediction variances correspond to the (i, i) th elements of $\mathbf{P}[k]$ for odd values of i .

B. Unified Tracking Example

As an example of typical tracking behavior, we demonstrate a Kalman filter tracker for the unified model specified in (8) and (10) for a system with $N_t = 20$ transmitters and $N_r = 10$ receivers. The state update interval was set to $T_0 = 0.250$ seconds and the carrier frequency was set to $\omega_c = 2\pi \cdot 900 \cdot 10^6$ radians/sec. All oscillators were assumed to have the same process noise parameters with $\alpha_t^{(n)} = \alpha_r^{(m)} = 2.31 \times 10^{-21}$ seconds and $\beta_t^{(n)} = \beta_r^{(m)} = 6.80 \times 10^{-23}$ Hertz for all n and

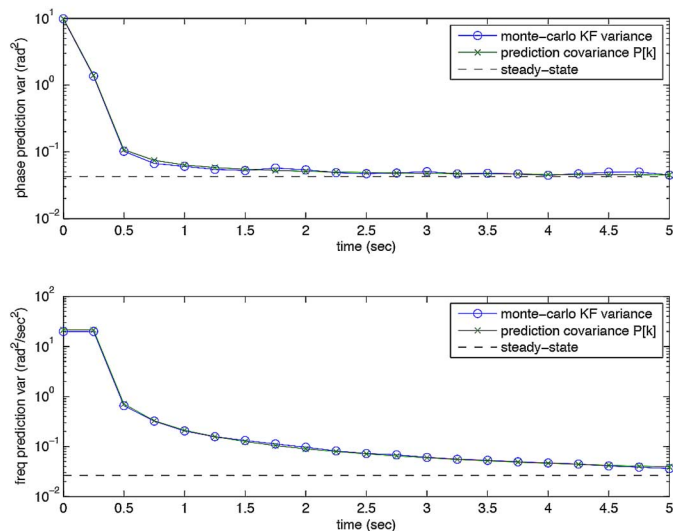


Fig. 3. Phase and frequency prediction variances for a Kalman filter tracker of the unified state-space model with $N_t = 20$, $N_r = 10$, and $T_0 = 0.250$.

m according to the Rakon RPFO45 oven-controlled oscillator parameters as discussed in Section II-A. The measurement noise variance was set to $r = (2\pi \cdot 10/360)^2 \text{ rad}^2$.

Fig. 3 plots the (1,1) and (2,2) elements of the prediction covariance matrix $\mathbf{P}[k]$, corresponding to the phase prediction variance and frequency prediction variance, respectively, versus the experimentally determined prediction variances obtained via Monte-Carlo simulation of the Kalman filter over 500 independent realizations of the initial states, process noises, and measurement noises. This example shows that the actual prediction variances of the Kalman filter agree with the corresponding elements of the prediction covariance matrix $\mathbf{P}[k]$ and that the prediction variances converge toward steady-state values. These values were obtained by solving a discrete-time algebraic Riccati equation. The following section formalizes the existence of the steady-state prediction covariance in the unified dynamic model and develops closed-form expressions for the asymptotic prediction covariance as $N_t \rightarrow \infty$ with $N_r = \eta N_t$.

C. Example Tracking and Feedback Implementation Strategies

In the context of coherent distributed MIMO communication systems, the purpose of channel tracking is to produce optimal channel predictions and to facilitate computation of precoding vectors for coherent distributed communication techniques, e.g., distributed beamforming and/or distributed nullforming. In the absence of channel reciprocity, some form of feedback from the receive nodes to the transmit nodes is required to facilitate coherent transmission. There are several ways in which the tracking system and feedback can be implemented. This section discusses two possible implementation strategies and their tradeoffs.

One possible implementation strategy is for the tracking and precoding vector calculations to be performed by a designated master receive node and for this receive node to feed back one or more precoding vectors to the transmit nodes. By exchanging messages among the receive nodes, the master receive node receives channel measurements from the other receive nodes, forms a complete copy of the observation vector $\mathbf{y}[k]$ containing

all $N_t N_r$ noisy channel phase measurements, generates channel predictions, computes the desired precoding vectors, and provides these precoding vectors to the transmit nodes via the feedback channel.

A second possible implementation strategy is for the receivers to feed back their observations and for one or more transmitters to perform the tracking. Since the observations at the receivers are broadcast back to the transmitters, each transmitter in the system will receive a complete copy of the observation vector $\mathbf{y}[k]$ containing all $N_t N_r$ noisy channel phase measurements. Each transmitter can then track the unified state $\delta[k]$, generate channel predictions, and compute precoding vectors individually without any additional information exchange between the transmitters. Alternatively, to avoid redundant computation, a master transmitter could be selected to perform the tracking and distribute precoding vector coefficients to the slave transmitters.

The first strategy has lower feedback requirements but requires centralized processing by a designated master receive node. The second strategy can be implemented without any messaging among the receive nodes or among the transmit nodes but has higher feedback requirements. While other implementation strategies are also possible, the particular choice of implementation strategy depends on the constraints and desired tradeoffs of the specific application. The analysis and numerical results in this paper do not depend on the particular tracking and feedback implementation strategy.

D. A Remark on Phase Unwrapping

While we have assumed the observations in (10) to be unwrapped phase measurements, it is usually the case in practical systems that only wrapped phase measurements are available. Additional considerations are often necessary in this case to avoid phase aliasing, incorrect phase unwrapping, and poor tracking performance.

The problem of tracking phases and frequencies in systems with wrapped phase measurements is well-known and results in an integer ambiguity in the noisy phase observations [35]. Several solutions have been proposed to work around this ambiguity, e.g., [38]–[41]. In practice, the effect of wrapped phase measurements is negligible if the standard deviation of the Kalman filter phase prediction error is small with respect to π . Since this is typically not the case during startup, one possible solution is to obtain accurate phase and frequency estimates [34] prior to tracking and to initialize the Kalman filter with predictions from these estimates. During steady-state operation, this also sets an upper limit on the observation interval T_0 since the steady-state phase prediction variance is an increasing function of T_0 .

IV. STEADY-STATE PREDICTION COVARIANCE ANALYSIS

In this section, we analyze the steady-state behavior of a Kalman filter tracker for the unified state $\delta[k]$. It is known that $[\mathbf{H}, \mathbf{F}]$ completely observable is sufficient for (13) to converge to a finite symmetric positive semidefinite steady-state covariance as $k \rightarrow \infty$ [35]. This steady-state covariance is not necessarily unique, however, and may depend on the initial covariance $\mathbf{P}[0]$. If, in addition, the system is such that $[\mathbf{F}, \mathbf{G}\mathbf{U}^{1/2}]$ is completely controllable, it is known that

with $\mathbf{Q}_0 = \mathbf{1}_{N_t} \mathbf{1}_{N_t}^\top \otimes \mathbf{q}$ and $\mathbf{Q}_1 = \mathbf{I}_{N_t} \otimes \mathbf{q}$ and where the final equality uses the Γ -notation established in (1).

If the measurement noise covariance also satisfies $\mathbf{R} = r \mathbf{I}_{N_t N_r}$, it is straightforward to see that every matrix $\{\mathbf{F}, \mathbf{H}, \mathbf{R}, \mathbf{Q}\}$ in the system as specified in (8) and (10) can be written in this Γ -notation. The following Theorem establishes that, when $\{\mathbf{F}, \mathbf{H}, \mathbf{R}, \mathbf{Q}\}$ can be expressed in this form (subject to observability), (14) can be efficiently solved by solving only two smaller DAREs.

Theorem 4: Given $[\mathbf{H}, \mathbf{F}]$ is completely observable and

$$\begin{aligned} \mathbf{F} &= \Gamma_n(\mathbf{F}_0, \mathbf{F}_1) \text{ with } \mathbf{F}_0 \in \mathbb{R}^{s \times s} \text{ and } \mathbf{F}_1 \in \mathbb{R}^{s \times s}, \\ \mathbf{H} &= \Gamma_n(\mathbf{H}_0, \mathbf{H}_1) \text{ with } \mathbf{H}_0 \in \mathbb{R}^{t \times s} \text{ and } \mathbf{H}_1 \in \mathbb{R}^{t \times s}, \\ \mathbf{R} &= \Gamma_n(\mathbf{R}_0, \mathbf{R}_1) \text{ with } \mathbf{R}_0 \in \mathbb{R}^{t \times t} \text{ and } \mathbf{R}_1 \in \mathbb{R}^{t \times t}, \text{ and} \\ \mathbf{Q} &= \Gamma_n(\mathbf{Q}_0, \mathbf{Q}_1) \text{ with } \mathbf{Q}_0 \in \mathbb{R}^{s \times s} \text{ and } \mathbf{Q}_1 \in \mathbb{R}^{s \times s} \end{aligned}$$

then the unique strong solution to (14) is given as $\mathbf{P} = \Gamma_n(\mathbf{P}_0, \mathbf{P}_1)$ with $\mathbf{P}_0 \in \mathbb{R}^{s \times s}$ the unique strong solution of

$$\mathbf{P}_0 = \mathbf{F}_0 \left[\mathbf{P}_0 - \mathbf{P}_0 \mathbf{H}_0^\top (\mathbf{H}_0 \mathbf{P}_0 \mathbf{H}_0^\top + \mathbf{R}_0)^{-1} \mathbf{H}_0 \mathbf{P}_0 \right] \mathbf{F}_0^\top + \mathbf{Q}_0$$

and $\bar{\mathbf{P}} = \mathbf{P}_0 + n \mathbf{P}_1 \in \mathbb{R}^{s \times s}$ the unique strong solution of

$$\bar{\mathbf{P}} = \bar{\mathbf{F}} \left[\bar{\mathbf{P}} - \bar{\mathbf{P}} \bar{\mathbf{H}}^\top (\bar{\mathbf{H}} \bar{\mathbf{P}} \bar{\mathbf{H}}^\top + \bar{\mathbf{R}})^{-1} \bar{\mathbf{H}} \bar{\mathbf{P}} \right] \bar{\mathbf{F}}^\top + \bar{\mathbf{Q}} \quad (21)$$

with $\bar{\mathbf{F}} := \mathbf{F}_0 + n \mathbf{F}_1$, $\bar{\mathbf{H}} := \mathbf{H}_0 + n \mathbf{H}_1$, $\bar{\mathbf{R}} := \mathbf{R}_0 + n \mathbf{R}_1$, and $\bar{\mathbf{Q}} := \mathbf{Q}_0 + n \mathbf{Q}_1$.

A proof of Theorem 4 is provided in Appendix B. Observe that the system specified in (8) and (10) satisfies the requirements of Theorem 4 with $n = N_r$. The utility of this theorem is that the $2N_t N_r \times 2N_t N_r$ DARE in (14) can be solved by computing two smaller $2N_t \times 2N_t$ DAREs, each of which is of lower dimension than the method described in Section IV-A. While the dimension of these smaller DAREs also grows without bound as $N_t \rightarrow \infty$, it turns out that we can further simplify the solution of (14) by observing that the system specified in (8) and (10) has the additional structure

$$\begin{aligned} \mathbf{F}_0 &= \Gamma_{N_t}(\mathbf{f}, \mathbf{0}) \\ \mathbf{H}_0 &= \Gamma_{N_t}(\mathbf{h}, \mathbf{0}) \\ \mathbf{R}_0 &= \Gamma_{N_t}(\mathbf{r}, \mathbf{0}) \\ \mathbf{Q}_0 &= \Gamma_{N_t}(\mathbf{0}, \mathbf{q}) \\ \mathbf{Q}_1 &= \Gamma_{N_t}(\mathbf{q}, \mathbf{0}) \end{aligned}$$

with $\mathbf{f} \in \mathbb{R}^{2 \times 2}$, $\mathbf{h} \in \mathbb{R}^{1 \times 2}$, $r \in \mathbb{R}$, and $\mathbf{q} \in \mathbb{R}^{2 \times 2}$ all defined in Section II-C. Hence, Theorem 4 can be *recursively* applied in the context of the oscillator tracking problem to say that $\mathbf{P} = \Gamma_{N_r}(\mathbf{P}_0, \mathbf{P}_1)$ with

$$\mathbf{P}_0 = \Gamma_{N_t}(\mathbf{p}_{00}, \mathbf{p}_{01}) \quad (22)$$

$$\mathbf{P}_1 = \Gamma_{N_t}(\mathbf{p}_{10}, \mathbf{p}_{11}) \quad (23)$$

where \mathbf{p}_{00} , \mathbf{p}_{01} , \mathbf{p}_{10} , and \mathbf{p}_{11} are all 2×2 matrices. This result implies that, irrespective of the number of transmit and receive nodes, the $2N_t N_r \times 2N_t N_r$ prediction covariance in (14) can be efficiently computed for the unified oscillator tracking problem by solving four 2×2 DAREs.

We can show that one of these 2×2 DAREs is trivial to solve in our unified oscillator tracking scenario. Recursively applying Theorem 4, we can write

$$\mathbf{p}_{00} = \mathbf{f} \left[\mathbf{p}_{00} - \mathbf{p}_{00} \mathbf{h}^\top (\mathbf{h} \mathbf{p}_{00} \mathbf{h}^\top + r)^{-1} \mathbf{h} \mathbf{p}_{00} \right] \mathbf{f}^\top + \mathbf{0}.$$

The unique solution to this DARE is $\mathbf{p}_{00} = \mathbf{0}$, which implies that $\mathbf{P}_0 = \Gamma_{N_t}(\mathbf{0}, \mathbf{p}_{01}) = \mathbf{1}_{N_t} \mathbf{1}_{N_t}^\top \otimes \mathbf{p}_{01}$. The remaining 2×2 constituent matrices \mathbf{p}_{10} , \mathbf{p}_{01} , and \mathbf{p}_{11} can be easily solved with numeric DARE solvers and then recombined to determine \mathbf{P}_0 , \mathbf{P}_1 , and \mathbf{P} .

V. ASYMPTOTIC PREDICTION COVARIANCE ANALYSIS

In this section, under the assumption that all nodes in the system have i.i.d. process and measurement noises, we develop closed-form expressions for the 2×2 constituent matrices \mathbf{p}_{10} , \mathbf{p}_{01} , and \mathbf{p}_{11} defined in (22) and (23) in the asymptotic regime where $N_t \rightarrow \infty$ and $N_r = \eta N_t$. This analysis leads to simple expressions for the elements in the steady-state prediction covariance matrix \mathbf{P} that, as shown in Section VI, can be good approximations of the actual steady-state prediction covariance even for modest values of N_t and N_r .

In the system defined in (8) and (10), we have $\mathbf{F}_1 = \mathbf{0}$, $\mathbf{H}_1 = \mathbf{0}$, and $\mathbf{R}_1 = \mathbf{0}$. We can define $\hat{\mathbf{P}} := N_r^{-1} \bar{\mathbf{P}}$ and $\hat{\mathbf{Q}} := N_r^{-1} \bar{\mathbf{Q}}$, and substitute $n = N_r$ to rewrite (21) as

$$\hat{\mathbf{P}} = \mathbf{F}_0 \left[\hat{\mathbf{P}} - \hat{\mathbf{P}} \mathbf{H}_0^\top (\mathbf{H}_0 \hat{\mathbf{P}} \mathbf{H}_0^\top + N_r^{-1} \mathbf{R}_0)^{-1} \mathbf{H}_0 \hat{\mathbf{P}} \right] \mathbf{F}_0^\top + \hat{\mathbf{Q}}. \quad (24)$$

As $N_r \rightarrow \infty$, we have $\hat{\mathbf{P}} \rightarrow \mathbf{P}_1$ and $\hat{\mathbf{Q}} \rightarrow \mathbf{Q}_1$. Hence, (24) becomes

$$\mathbf{P}_1 = \mathbf{F}_0 \left[\mathbf{P}_1 - \mathbf{P}_1 \mathbf{H}_0^\top (\mathbf{H}_0 \mathbf{P}_1 \mathbf{H}_0^\top)^{-1} \mathbf{H}_0 \mathbf{P}_1 \right] \mathbf{F}_0^\top + \mathbf{Q}_1.$$

Since $\mathbf{Q}_1 = \mathbf{I}_{N_t} \otimes \mathbf{q}$, $\mathbf{F}_0 = \mathbf{I}_{N_t} \otimes \mathbf{f}$, and $\mathbf{H}_0 = \mathbf{I}_{N_t} \otimes \mathbf{h}$ are all block diagonal matrices, it is straightforward to see that the asymptotic value of \mathbf{P}_1 is also block diagonal. In other words, $\mathbf{P}_1 \rightarrow \mathbf{I}_{N_t} \otimes \mathbf{p}_{10}$ and $\mathbf{p}_{11} \rightarrow \mathbf{0}$. Hence, to determine \mathbf{P}_1 for large N_r , it is only necessary to solve the 2×2 DARE

$$\mathbf{p}_{10} = \mathbf{f} \left[\mathbf{p}_{10} - \mathbf{p}_{10} \mathbf{h}^\top (\mathbf{h} \mathbf{p}_{10} \mathbf{h}^\top)^{-1} \mathbf{h} \mathbf{p}_{10} \right] \mathbf{f}^\top + \mathbf{q}. \quad (25)$$

Now consider $\mathbf{P}_0 = \mathbf{1}_{N_t} \mathbf{1}_{N_t}^\top \otimes \mathbf{p}_{01}$. Defining $\hat{\mathbf{p}}_{01} = N_t^{-1} \mathbf{p}_{00} + \mathbf{p}_{01}$, we have that $\hat{\mathbf{p}}_{01} = \mathbf{p}_{01}$ since, as shown previously, $\mathbf{p}_{00} = \mathbf{0}$ for any N_t and N_r . Theorem 4 implies that \mathbf{p}_{01} satisfies

$$\mathbf{p}_{01} = \mathbf{f} \left[\mathbf{p}_{01} - \mathbf{p}_{01} \mathbf{h}^\top (\mathbf{h} \mathbf{p}_{01} \mathbf{h}^\top + N_r^{-1} r)^{-1} \mathbf{h} \mathbf{p}_{01} \right] \mathbf{f}^\top + \mathbf{q}$$

which, in the limit as $N_r \rightarrow \infty$, is identical in form to (25). Hence, in the asymptotic regime where $N_t \rightarrow \infty$ and $N_r = \eta N_t$, we have $\mathbf{p}_{01} = \mathbf{p}_{10} = \mathbf{p}$ with \mathbf{p} satisfying the 2×2 DARE

$$\mathbf{p} = \mathbf{f} \left[\mathbf{p} - \mathbf{p} \mathbf{h}^\top (\mathbf{h} \mathbf{p} \mathbf{h}^\top)^{-1} \mathbf{h} \mathbf{p} \right] \mathbf{f}^\top + \mathbf{q}. \quad (26)$$

In other words, it is only necessary to solve a *single* 2×2 DARE to fully characterize the $2N_t N_r \times 2N_t N_r$ asymptotic prediction covariance matrix \mathbf{P} .

Summarizing these results, we have $\mathbf{p}_{00} = \mathbf{0}$, $\mathbf{p}_{11} \rightarrow \mathbf{0}$, $\mathbf{p}_{01} \rightarrow \mathbf{p}$, and $\mathbf{p}_{10} \rightarrow \mathbf{p}$ as $N_t \rightarrow \infty$ with $N_r = \eta N_t$. Hence,

$$\mathbf{P}_0 \rightarrow \mathbf{\Gamma}_{N_t}(\mathbf{0}, \mathbf{p}) \quad (27)$$

$$\mathbf{P}_1 \rightarrow \mathbf{\Gamma}_{N_t}(\mathbf{p}, \mathbf{0}) \quad (28)$$

with \mathbf{p} satisfying (26) and the asymptotic prediction covariance $\mathbf{P} = \mathbf{\Gamma}_n(\mathbf{P}_0, \mathbf{P}_1)$ taking the same form as (20) with \mathbf{q} replaced by \mathbf{p} .

To compute closed-form expressions for the elements of \mathbf{p} , we denote

$$\mathbf{p} = \begin{bmatrix} p(1, 1) & p(1, 2) \\ p(2, 1) & p(2, 2) \end{bmatrix}$$

and, from (5) under the assumption of identical process noise statistics at each receive node, set

$$\mathbf{q} = \omega_c^2 T_0 \begin{bmatrix} \alpha + \beta \frac{T_0^2}{3} & \beta \frac{T_0}{2} \\ \beta \frac{T_0}{2} & \beta \end{bmatrix}.$$

Some straightforward algebra on (26) yields

$$p(1, 2) = p(2, 1) = \omega_c^2 T_0^2 \beta \left(\gamma + \frac{1}{2} \right)$$

with $\gamma := \sqrt{\frac{1}{12} + \frac{\alpha}{T_0^2 \beta}}$. The remaining elements of \mathbf{p} follow as

$$\begin{aligned} p(1, 1) &= \omega_c^2 T_0^3 \beta \left(\gamma + \frac{1}{2} \right)^2 \\ p(2, 2) &= \omega_c^2 T_0 \beta (\gamma + 1). \end{aligned}$$

Note that the asymptotic prediction covariance is not a function of $\eta = \frac{N_r}{N_t}$ or the measurement noise variance r . The asymptotic prediction covariance is only a function of the i.i.d. process noise parameters α and β as well as the carrier frequency ω_c and the update period T_0 . The parameter η only affects the rate at which the elements of the prediction covariance matrix approach their asymptotic values, as shown in Section VI.

VI. NUMERICAL RESULTS

This section presents numerical results confirming the asymptotic analysis in Section V and also demonstrating the advantages of unified tracking in a scenario with simultaneous beamforming and nullforming. All of the results in this section assume a measurement noise standard deviation of 10 degrees, corresponding to $r = (2\pi \cdot 10/360)^2 \text{ rad}^2$. Since there are only 12 unique elements in the prediction covariance matrix \mathbf{P} irrespective of the number of transmit and receive nodes, Table I lists the 12 relevant elements of \mathbf{P} , their meanings, and their asymptotic values.

Fig. 4 plots elements of the prediction covariance matrix \mathbf{P} versus the number of transmit nodes N_t with $N_r = \eta N_t$ and $\eta = 0.2$. The simulation parameters are otherwise identical to those in Section III ($T_0 = 0.250$ seconds, $\omega_c = 2\pi \cdot 900 \cdot 10^6$ radians/sec, $\alpha_t^{(n)} = \alpha_r^{(m)} = 2.31 \times 10^{-21}$ seconds, and $\beta_t^{(n)} = \beta_r^{(m)} = 6.80 \times 10^{-23}$ Hertz for all n and m). These results confirm the asymptotic analysis in Section V and show that asymptotic results can be accurate predictions of many of

TABLE I
UNIQUE ELEMENTS OF THE PREDICTION COVARIANCE MATRIX \mathbf{P} WITH $n' \neq n$ AND $m' \neq m$.

$\mathbf{P}(i, j)$	Meaning and asymptotic value
$\mathbf{P}(1, 1)$	Phase var $\text{cov}(\phi^{(n,m)}, \phi^{(n,m)}) \rightarrow 2p(1, 1)$
$\mathbf{P}(1, 2)$	Phase/freq cov $\text{cov}(\phi^{(n,m)}, \omega^{(n,m)}) \rightarrow 2p(1, 2)$
$\mathbf{P}(2, 2)$	Frequency var $\text{cov}(\omega^{(n,m)}, \omega^{(n,m)}) \rightarrow 2p(2, 2)$
$\mathbf{P}(3, 1)$	Phase cov $\text{cov}(\phi^{(n,m)}, \phi^{(n',m')}) \rightarrow p(1, 1)$
$\mathbf{P}(3, 2)$	Phase/freq cov $\text{cov}(\phi^{(n,m)}, \omega^{(n',m')}) \rightarrow p(1, 2)$
$\mathbf{P}(4, 2)$	Frequency var $\text{cov}(\omega^{(n,m)}, \omega^{(n',m')}) \rightarrow p(2, 2)$
$\mathbf{P}(2N_t + 1, 1)$	Phase cov $\text{cov}(\phi^{(n,m)}, \phi^{(n,m')}) \rightarrow p(1, 1)$
$\mathbf{P}(2N_t + 1, 2)$	Phase/freq cov $\text{cov}(\phi^{(n,m)}, \omega^{(n,m')}) \rightarrow p(1, 2)$
$\mathbf{P}(2N_t + 2, 2)$	Frequency var $\text{cov}(\omega^{(n,m)}, \omega^{(n,m')}) \rightarrow p(2, 2)$
$\mathbf{P}(2N_t + 3, 1)$	Phase cov $\text{cov}(\phi^{(n,m)}, \phi^{(n',m')}) \rightarrow 0$
$\mathbf{P}(2N_t + 3, 2)$	Phase/freq cov $\text{cov}(\phi^{(n,m)}, \omega^{(n',m')}) \rightarrow 0$
$\mathbf{P}(2N_t + 4, 2)$	Frequency var $\text{cov}(\omega^{(n,m)}, \omega^{(n',m')}) \rightarrow 0$

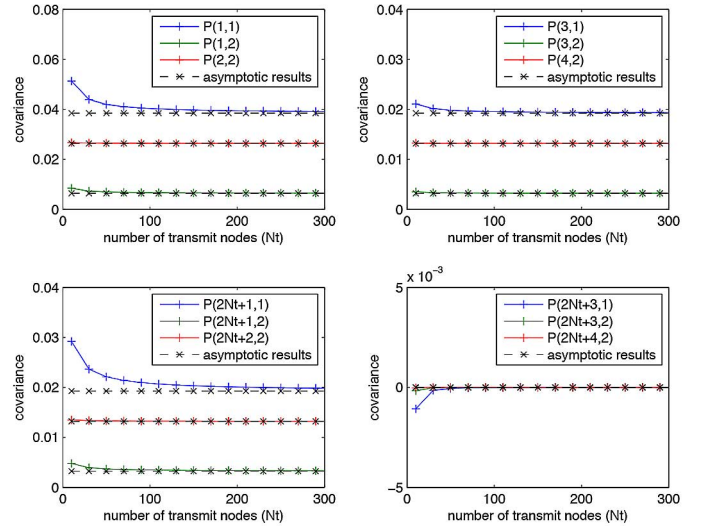


Fig. 4. Relevant elements of the prediction covariance matrix versus the number of transmit nodes N_t with $N_r = \eta N_t$ and $\eta = 0.2$.

the elements of the prediction covariance matrix even for small values of N_t and N_r .

Fig. 5 repeats the results in Fig. 4 with $\eta = 1$. As predicted in Section V, the asymptotic results are unaffected by η . The main difference in these results with respect to those in Fig. 4 are that the elements of the prediction covariance matrix converge more quickly to their asymptotic values since N_r is larger for each value of N_t . Also note that the covariances $\mathbf{P}(2N_t + 1, 1)$, $\mathbf{P}(2N_t + 1, 2)$, and $\mathbf{P}(2N_t + 2, 2)$ converge at the same rate as $\mathbf{P}(3, 1)$, $\mathbf{P}(3, 2)$, and $\mathbf{P}(4, 2)$ in this example. This is a consequence of the fact that $N_t = N_r$ in this system.

In both Figs. 4 and 5, observe that the steady-state phase prediction variance $P(1, 1) \leq 0.06 \text{ rad}^2$ in all of the cases considered. This corresponds to a phase prediction standard deviation of less than $0.08 \cdot \pi$, implying that the probability of phase aliasing (cycle slips) from wrapped phase measurements during steady-state operation of the Kalman filter is small in these examples.

Fig. 6 plots the asymptotic phase standard deviation (in degrees) versus oscillator parameters α and β for

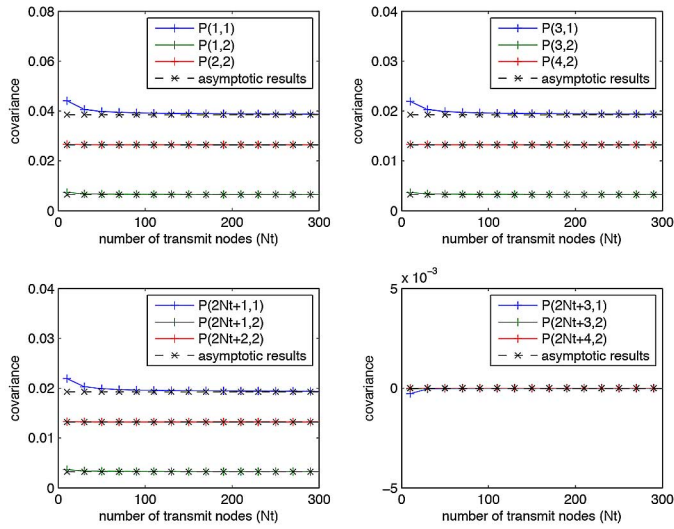


Fig. 5. Relevant elements of the covariance matrix versus the number of transmit nodes N_t with $N_r = \eta N_t$ and $\eta = 1$.

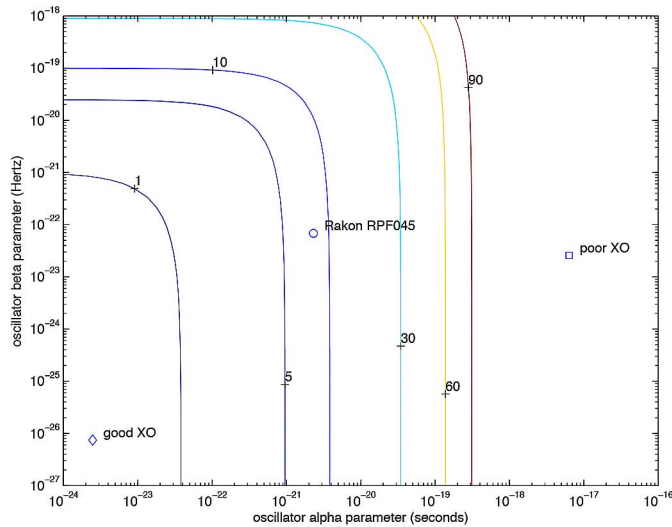


Fig. 6. Asymptotic phase standard deviation (in degrees) versus oscillator parameters α and β for $T_0 = 0.250$ seconds and $\omega_c = 2\pi \cdot 900 \cdot 10^6$ radians/sec.

$T_0 = 0.250$ seconds and $\omega_c = 2\pi \cdot 900 \cdot 10^6$ radians/sec. Specifically, this plot shows $\frac{360}{2\pi} \cdot \sqrt{p(1,1)}$ over a range of typical oscillator parameters with “good XO” and “poor XO” oscillator parameters fitted to a table of typical Allan variances from [33]. These results show that a system using the Rakon oven-controlled oscillators with $T_0 = 0.250$ seconds and $\omega_c = 2\pi \cdot 900 \cdot 10^6$ radians/sec will have an asymptotic phase prediction standard deviation of less than 10 degrees, which is more than adequate to achieve good coherent beamforming gains but may be insufficient to achieve deep nulls [9]. The “poor XO” has an asymptotic phase prediction standard deviation so large that coherent distributed transmission is impossible. To achieve coherent transmission with the “poor XO”, the carrier frequency ω_c and/or the measurement interval T_0 must be reduced.

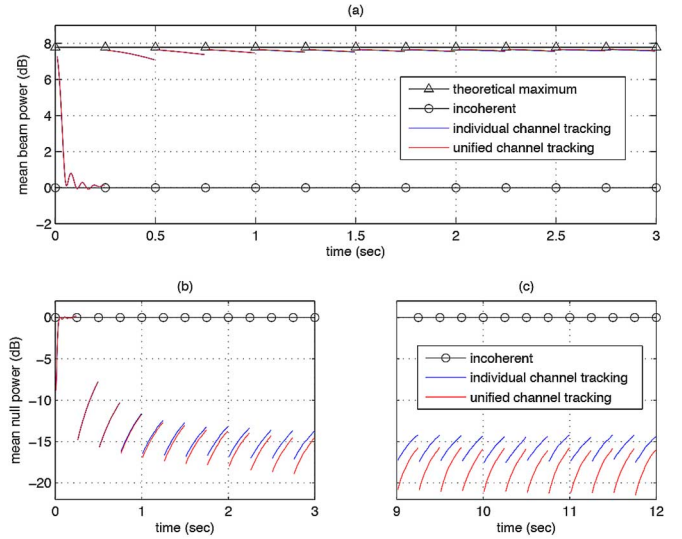


Fig. 7. Beamforming (subfigure (a)) and nullforming (subfigures (b) and (c)) performance for a distributed MIMO system with $N_t = 10$ transmitters and $N_r = 5$ receivers. Nulls are steered toward four receivers and a beam is steered toward the fifth receiver.

To demonstrate the performance of unified tracking in a communications setting, we consider a scenario where the distributed transmit array forms nulls toward $N_r - 1$ “protected” receivers and uses the remaining degrees of freedom to form a beam and maximize the power at the remaining “intended” receiver. The phase predictions from the Kalman filter are used in conjunction with the known channel amplitudes to calculate a time-varying zero-forcing linear precoding vector as described in [9]. All channels are assumed to have unit magnitude and the transmit array is assumed to have a unit total power constraint.

Fig. 7 shows the distributed beamforming and nullforming performance of a system with $N_t = 10$ transmitters, $N_r = 5$ receivers, and a measurement interval $T_0 = 250$ ms. Results are shown for “individual tracking” in which each pairwise channel is tracked in a separate two-state Kalman filter versus “unified tracking” as described in Section II-C. The results were averaged over 2000 realizations of the random initial frequency offsets, clock process noises, and measurement noises. Measurements occur at $t = kT_0$ for $k = 0, 1, \dots$

Subfigure (a) of Fig. 7 shows the beamforming performance. Due to the relatively poor frequency estimates of the Kalman filters after the first measurement at $t = 0$, the beam is effectively incoherent on $0 < t < 0.25$. After the second measurement at $t = 0.25$, the Kalman filter state estimates and the resulting beam power improves and approaches the theoretical maximum $10 \log_{10} (N_t (1 - (N_r - 1)/N_t)) \approx 7.8$ dB. As t increases in the beamforming interval $0.25 < t < 0.50$, the channel predictions become increasingly stale and the resulting beamforming performance degrades slightly by the end of the beamforming interval. In this example, the beamforming performance approaches its steady-state behavior after only a few measurement intervals and the performance of individual and unified channel tracking is effectively identical.

Subfigures (b) and (c) of Fig. 7 show the nullforming performance with subfigure (b) showing the transient behavior on $0 < t < 3$ and subfigure (c) showing the steady-state behavior

on $9 < t < 12$. As with beamforming, the nulls are effectively incoherent after one measurement on the interval $0 < t < 0.25$. The null powers improve with subsequent measurements and the effect of stale channel predictions is more pronounced than with beamforming. Subfigure (c) shows that unified tracking can provide a potentially significant advantage in nullforming gain with nulls 3–4 dB deeper than with individual channel tracking in this example.

VII. CONCLUSION

This paper presented a formal analysis of the stability and steady-state behavior of a Kalman filter tracker for the effective channel states in an unsynchronized distributed MIMO system. While the state-space system was shown to be nonstabilizable, the Kalman filter tracker was shown to be asymptotically stable subject to a properly chosen initial prediction covariance. A unique “strong” solution to the steady-state prediction covariance was also shown to exist and two methods were developed to efficiently solve for this unique strong solution. An asymptotic analysis was also presented for large networks with closed-form results for all of the elements in the asymptotic prediction covariance matrix. Numeric results confirmed the analysis and demonstrated the effect of the oscillator parameters on the ability of the system to achieve coherent transmission.

APPENDIX A PROOF OF THEOREM 3

We first establish the existence and uniqueness of a positive definite $\mathbf{\Pi}$ satisfying (19) by showing that $[\mathbf{A}_1, \mathbf{B}_1]$ is completely controllable and $[\mathbf{C}_1, \mathbf{A}_1]$ is completely observable. The former result follows directly from the construction of the controllable staircase form. The latter result is shown below.

From Lemma 1, we know $[\mathbf{H}, \mathbf{F}]$ is completely observable. Moreover, since complete observability is invariant to a similarity transform, $[\mathbf{H}, \mathbf{F}]$ completely observable implies $[\mathbf{C}, \mathbf{A}]$ is also completely observable. The Popov-Belevitch-Hautus (PBH) test for observability [44] then implies that

$$\text{rank} \left(\begin{bmatrix} \lambda \mathbf{I} - \mathbf{A} \\ \mathbf{C} \end{bmatrix} \right) = \text{rank}(\mathbf{A}). \quad (29)$$

To establish a contradiction, suppose $[\mathbf{C}_1, \mathbf{A}_1]$ is not completely observable. The PBH test then implies that there exists a scalar λ and a nonzero vector \mathbf{z} such that

$$\begin{bmatrix} \lambda \mathbf{I} - \mathbf{A}_1 \\ \mathbf{C}_1 \end{bmatrix} \mathbf{z} = \mathbf{0}.$$

It follows that

$$\begin{bmatrix} \lambda \mathbf{I} - \mathbf{A}_1 & -\mathbf{A}_2 \\ \mathbf{0} & \lambda \mathbf{I} - \mathbf{A}_3 \\ \mathbf{C}_1 & \mathbf{C}_2 \end{bmatrix} \begin{bmatrix} \mathbf{z} \\ \mathbf{0} \end{bmatrix} = \mathbf{0}.$$

Thus

$$\text{rank} \left(\begin{bmatrix} \lambda \mathbf{I} - \mathbf{A} \\ \mathbf{C} \end{bmatrix} \right) < \text{rank}(\mathbf{A})$$

which contradicts (29). Hence, $[\mathbf{C}_1, \mathbf{A}_1]$ is completely observable and, in light of the complete controllability of $[\mathbf{A}_1, \mathbf{B}_1]$, there exists a unique positive definite $\mathbf{\Pi}$ satisfying (19). Moreover, this unique positive definite $\mathbf{\Pi}$ satisfying (19) is stabilizing for $\{\mathbf{A}_1, \mathbf{B}_1, \mathbf{C}_1, \mathbf{R}\}$ [42].

Observe that $\mathbf{\Pi}$ positive definite implies $\bar{\mathbf{\Pi}}$ as defined in (18) is positive semidefinite. We now show that $\bar{\mathbf{\Pi}}$ as defined in (18) satisfies the DARE for $\{\mathbf{A}, \mathbf{B}, \mathbf{C}, \mathbf{R}\}$. This can be seen by writing

$$\begin{aligned} & \mathbf{A} \left(\bar{\mathbf{\Pi}} - \bar{\mathbf{\Pi}} \mathbf{C}^\top \left(\mathbf{C} \bar{\mathbf{\Pi}} \mathbf{C}^\top + \mathbf{R} \right)^{-1} \mathbf{C} \bar{\mathbf{\Pi}} \right) \mathbf{A}^\top + \mathbf{B} \mathbf{B}^\top \\ &= \mathbf{A} \left(\bar{\mathbf{\Pi}} - \begin{bmatrix} \mathbf{\Pi} \mathbf{C}_1^\top \\ \mathbf{0} \end{bmatrix} \right) \left(\mathbf{C}_1 \mathbf{\Pi} \mathbf{C}_1^\top + \mathbf{R} \right)^{-1} \begin{bmatrix} \mathbf{\Pi} \mathbf{C}_1 & \mathbf{0} \end{bmatrix} \mathbf{A}^\top + \mathbf{B} \mathbf{B}^\top \\ &= \mathbf{A} \begin{bmatrix} \mathbf{\Pi} - \mathbf{\Pi} \mathbf{C}_1^\top \left(\mathbf{C}_1 \mathbf{\Pi} \mathbf{C}_1^\top + \mathbf{R} \right)^{-1} \mathbf{C}_1 \mathbf{\Pi} & \mathbf{0} \\ \mathbf{0} & \mathbf{0} \end{bmatrix} \mathbf{A}^\top + \begin{bmatrix} \mathbf{B}_1 \mathbf{B}_1^\top & \mathbf{0} \\ \mathbf{0} & \mathbf{0} \end{bmatrix} \\ &= \begin{bmatrix} \mathbf{A}_1 \left(\mathbf{\Pi} - \mathbf{\Pi} \mathbf{C}_1^\top \left(\mathbf{C}_1 \mathbf{\Pi} \mathbf{C}_1^\top + \mathbf{R} \right)^{-1} \mathbf{C}_1 \mathbf{\Pi} \right) \mathbf{A}_1^\top + \mathbf{B}_1 \mathbf{B}_1^\top & \mathbf{0} \\ \mathbf{0} & \mathbf{0} \end{bmatrix} \\ &= \begin{bmatrix} \mathbf{\Pi} & \mathbf{0} \\ \mathbf{0} & \mathbf{0} \end{bmatrix} \\ &= \bar{\mathbf{\Pi}}. \end{aligned}$$

Thus, by construction, $\bar{\mathbf{\Pi}}$ is a symmetric positive semidefinite matrix that satisfies the DARE for $\{\mathbf{A}, \mathbf{B}, \mathbf{C}, \mathbf{R}\}$. Consequently, $\mathbf{P} = \mathbf{T}^{-1} \bar{\mathbf{\Pi}} \mathbf{T}^{-\top}$ is a symmetric positive semidefinite matrix that satisfies (14).

Finally, we will show that $\mathbf{P} = \mathbf{T}^{-1} \bar{\mathbf{\Pi}} \mathbf{T}^{-\top}$ is a strong solution, and hence is the unique strong solution to (14). The eigenvalues of \mathbf{E} in (15) are invariant to similarity transformation, hence we can write

$$\begin{aligned} \mathbf{T} \mathbf{E} \mathbf{T}^{-1} &= \mathbf{T} \mathbf{F} \mathbf{T}^{-1} - \mathbf{T} \mathbf{F} \mathbf{P} \mathbf{H}^\top \left(\mathbf{H} \mathbf{P} \mathbf{H}^\top + \mathbf{R} \right)^{-1} \mathbf{H} \mathbf{T}^{-1} \\ &= \mathbf{A} - \mathbf{A} \bar{\mathbf{\Pi}} \mathbf{C}^\top \left(\mathbf{C} \bar{\mathbf{\Pi}} \mathbf{C}^\top + \mathbf{R} \right)^{-1} \mathbf{C} \\ &= \begin{bmatrix} \mathbf{A}_1 - \mathbf{A}_1 \mathbf{\Pi} \mathbf{C}_1^\top \left(\mathbf{C}_1 \mathbf{\Pi} \mathbf{C}_1^\top + \mathbf{R} \right)^{-1} \mathbf{C}_1 & \mathbf{X} \\ \mathbf{0} & \mathbf{A}_3 \end{bmatrix} \end{aligned}$$

where \mathbf{X} is inconsequential to the eigenvalues of \mathbf{E} . Since $\mathbf{\Pi}$ is stabilizing for $\{\mathbf{A}_1, \mathbf{B}_1, \mathbf{C}_1, \mathbf{R}\}$, the eigenvalues of $\mathbf{A}_1 - \mathbf{A}_1 \mathbf{\Pi} \mathbf{C}_1^\top \left(\mathbf{C}_1 \mathbf{\Pi} \mathbf{C}_1^\top + \mathbf{R} \right)^{-1} \mathbf{C}_1$ must all have magnitude in the open unit disk. The matrix \mathbf{A}_3 has eigenvalues all equal to one. Hence $\max |\lambda(\mathbf{E})| = 1$ and $\mathbf{P} = \mathbf{T}^{-1} \bar{\mathbf{\Pi}} \mathbf{T}^{-\top}$ is the unique strong solution to (14).

APPENDIX B PROOF OF THEOREM 4

Consider the matrix $\mathbf{\Gamma}_n(0, 1) = \mathbf{1}_n \mathbf{1}_n^\top$. This matrix has an eigenvalue at zero with algebraic multiplicity $n-1$ and an eigenvalue at n corresponding to the eigenvector $\mathbf{1}_n$. Since $\mathbf{\Gamma}_n(0, 1)$ is real and symmetric, it is diagonalizable and there exists \mathbf{T} such that

$$\mathbf{T}^{-1} \mathbf{\Gamma}_n(0, 1) \mathbf{T} = \text{diag}(0, \dots, 0, n). \quad (30)$$

Now let $\mathbf{T}_s = \mathbf{T} \otimes \mathbf{I}_s$ and $\mathbf{T}_t = \mathbf{T} \otimes \mathbf{I}_t$. For general \mathbf{A} and \mathbf{B} , both $t \times s$ matrices, we can write

$$\begin{aligned} \mathbf{T}_s^{-1} \mathbf{\Gamma}_n(\mathbf{A}, \mathbf{B}) \mathbf{T}_t &= (\mathbf{T} \otimes \mathbf{I}_s)^{-1} (\mathbf{I}_n \otimes \mathbf{A} + \mathbf{1}_n \mathbf{1}_n^\top \otimes \mathbf{B}) (\mathbf{T} \otimes \mathbf{I}_t) \\ &= (\mathbf{T}^{-1} \otimes \mathbf{A} + \mathbf{T}^{-1} \mathbf{1}_n \mathbf{1}_n^\top \otimes \mathbf{B}) (\mathbf{T} \otimes \mathbf{I}_t) \\ &= \mathbf{I}_n \otimes \mathbf{A} + (\mathbf{T}^{-1} \mathbf{1}_n \mathbf{1}_n^\top \mathbf{T}) \otimes \mathbf{B} \\ &= \mathbf{I}_n \otimes \mathbf{A} + (\text{diag}(0, \dots, 0, n)) \otimes \mathbf{B} \\ &= \text{blockdiag}(\mathbf{A}, \dots, \mathbf{A}, \mathbf{A} + n\mathbf{B}) \end{aligned}$$

where the second to last equality used (30).

When $t = s$, the matrices \mathbf{A} and \mathbf{B} are square and $\mathbf{T}_s^{-1}\mathbf{T}_n(\mathbf{A}, \mathbf{B})\mathbf{T}_t = \text{blockdiag}(\mathbf{A}, \dots, \mathbf{A}, \mathbf{A} + n\mathbf{B})$ is a similarity transformation. Now defining,

$$\begin{aligned}\tilde{\mathbf{F}} &:= \mathbf{T}_s^{-1}\mathbf{F}\mathbf{T}_s = \text{blockdiag}(\mathbf{F}_0, \dots, \mathbf{F}_0, \mathbf{F}_0 + n\mathbf{F}_1) \\ \tilde{\mathbf{H}} &:= \mathbf{T}_t^{-1}\mathbf{H}\mathbf{T}_s = \text{blockdiag}(\mathbf{H}_0, \dots, \mathbf{H}_0, \mathbf{H}_0 + n\mathbf{H}_1) \\ \tilde{\mathbf{R}} &:= \mathbf{T}_t^{-1}\mathbf{R}\mathbf{T}_t = \text{blockdiag}(\mathbf{R}_0, \dots, \mathbf{R}_0, \mathbf{R}_0 + n\mathbf{R}_1) \\ \tilde{\mathbf{Q}} &:= \mathbf{T}_s^{-1}\mathbf{Q}\mathbf{T}_s = \text{blockdiag}(\mathbf{Q}_0, \dots, \mathbf{Q}_0, \mathbf{Q}_0 + n\mathbf{Q}_1) \\ \tilde{\mathbf{P}} &:= \mathbf{T}_s^{-1}\mathbf{P}\mathbf{T}_s = \text{blockdiag}(\mathbf{P}_0, \dots, \mathbf{P}_0, \mathbf{P}_0 + n\mathbf{P}_1)\end{aligned}$$

we can apply this similarity transformation to rewrite (14) as

$$\tilde{\mathbf{P}} = \tilde{\mathbf{F}} \left[\tilde{\mathbf{P}} - \tilde{\mathbf{H}}\tilde{\mathbf{H}}^\top (\tilde{\mathbf{H}}\tilde{\mathbf{P}}\tilde{\mathbf{H}}^\top + \tilde{\mathbf{R}})^{-1} \tilde{\mathbf{H}}\tilde{\mathbf{P}} \right] \tilde{\mathbf{F}}^\top + \tilde{\mathbf{Q}}. \quad (31)$$

Since $[\mathbf{H}, \mathbf{F}]$ is completely observable, it is also detectable. Moreover, since detectability is invariant to a similarity transform, $[\mathbf{H}, \mathbf{F}]$ detectable implies $[\tilde{\mathbf{H}}, \tilde{\mathbf{F}}]$ is detectable. Hence there exists a unique strong solution $\tilde{\mathbf{P}}$ to (31) as shown in [42, Theorem 3.1].

Due to the block diagonal nature all of the matrices in (31), the transformed system can be viewed as n uncoupled systems, each with s states. Observe that $n - 1$ of these systems have identical dynamics. Hence, there are only two distinct $s \times s$ DAREs to solve. The first DARE is given as

$$\mathbf{P}_0 = \mathbf{F}_0 \left[\mathbf{P}_0 - \mathbf{P}_0 \mathbf{H}_0^\top (\mathbf{H}_0 \mathbf{P}_0 \mathbf{H}_0^\top + \mathbf{R}_0)^{-1} \mathbf{H}_0 \mathbf{P}_0 \right] \mathbf{F}_0^\top + \mathbf{Q}_0.$$

Denoting $\bar{\mathbf{P}} = \mathbf{P}_0 + n\mathbf{P}_1$ and using similar notation for the other relevant matrices, the second DARE can be written as

$$\bar{\mathbf{P}} = \bar{\mathbf{F}} \left[\bar{\mathbf{P}} - \bar{\mathbf{P}}\bar{\mathbf{H}}^\top (\bar{\mathbf{H}}\bar{\mathbf{P}}\bar{\mathbf{H}}^\top + \bar{\mathbf{R}})^{-1} \bar{\mathbf{H}}\bar{\mathbf{P}} \right] \bar{\mathbf{F}}^\top + \bar{\mathbf{Q}}.$$

Finally, note that both \mathbf{P}_0 and $\bar{\mathbf{P}}$ must be strong since $\tilde{\mathbf{P}} = \text{blockdiag}(\mathbf{P}_0, \dots, \mathbf{P}_0, \bar{\mathbf{P}})$ is strong if and only if \mathbf{P}_0 and $\bar{\mathbf{P}}$ are both strong.

REFERENCES

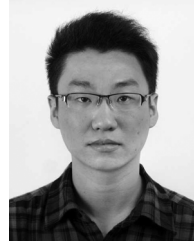
- [1] R. Mudumbai, G. Barriac, and U. Madhow, "On the feasibility of distributed beamforming in wireless networks," *IEEE Trans. Wireless Commun.*, vol. 6, no. 5, pp. 1754–1763, May 2007.
- [2] D. R. Brown, III, U. Madhow, P. Bidigare, and S. Dasgupta, "Receiver-coordinated distributed transmit nullforming with channel state uncertainty," in *Proc. 46th Annu. Conf. Inf. Sci. Syst. (CISS)*, Mar. 21–23, 2012, pp. 1–6.
- [3] K. Zarifi, S. Affes, and A. Ghayeb, "Collaborative null-steering beamforming for uniformly distributed wireless sensor networks," *IEEE Trans. Signal Process.*, vol. 58, no. 3, pp. 1889–1903, Mar. 2010.
- [4] Y. Tu and G. Pottie, "Coherent cooperative transmission from multiple adjacent antennas to a distant stationary antenna through AWGN channels," in *Proc. IEEE Veh. Technol. Conf. (VTC)*, Birmingham, AL, USA, May 2002, vol. 1, pp. 130–134.
- [5] R. Irmer, H. Droste, P. Marsch, M. Grieger, G. Fettweis, S. Brueck, H.-P. Mayer, L. Thiele, and V. Jungnickel, "Coordinated multipoint: concepts, performance, and field trial results," *IEEE Commun. Mag.*, vol. 49, no. 2, pp. 102–111, Feb. 2011.
- [6] D. Brown, P. Bidigare, and U. Madhow, "Receiver-coordinated distributed transmit beamforming with kinematic tracking," in *Proc. IEEE Int. Conf. Acoust., Speech, Signal Process. (ICASSP)*, Mar. 2012, pp. 5209–5212.
- [7] D. Brown, R. Mudumbai, and S. Dasgupta, "Fundamental limits on phase and frequency tracking and estimation in drifting oscillators," in *Proc. IEEE Int. Conf. Acoust., Speech, Signal Process. (ICASSP)*, Mar. 2012, pp. 5225–5228.
- [8] D. R. Brown, III, P. Bidigare, S. Dasgupta, and U. Madhow, "Receiver-coordinated zero-forcing distributed transmit nullforming," in *Proc. IEEE Statist. Signal Process. Workshop (SSP)*, Aug. 2012, pp. 269–272.
- [9] R. Brown, III and R. David, "Receiver-coordinated distributed transmit nullforming with local and unified tracking," in *Proc. IEEE Int. Conf. Acoust., Speech, Signal Process. (ICASSP)*, May 2014, pp. 1160–1164.
- [10] R. Mudumbai, J. Hespanha, U. Madhow, and G. Barriac, "Scalable feedback control for distributed beamforming in sensor networks," in *Proc. IEEE Int. Symp. Inf. Theory (ISIT)*, Adelaide, Australia, Sep. 2005, pp. 137–141.
- [11] R. Mudumbai, B. Wild, U. Madhow, and K. Ramchandran, "Distributed beamforming using 1 bit feedback: from concept to realization," in *Proc. 44th Allerton Conf. Commun., Control, Comput.*, Monticello, IL, USA, Sep. 2006, pp. 1020–1027.
- [12] R. Mudumbai, J. Hespanha, U. Madhow, and G. Barriac, "Distributed transmit beamforming using feedback control," *IEEE Trans. Inf. Theory*, vol. 56, no. 1, pp. 411–426, Jan. 2010.
- [13] I. Ozil and D. R. Brown, III, "Time-slotted round-trip carrier synchronization," in *Proc. 41st Asilomar Conf. Signals, Syst., Comput.*, Pacific Grove, CA, USA, Nov. 4–7, 2007, pp. 1781–1785.
- [14] D. R. Brown, III and H. V. Poor, "Time-slotted round-trip carrier synchronization for distributed beamforming," *IEEE Trans. Signal Process.*, vol. 56, no. 11, pp. 5630–5643, Nov. 2008.
- [15] D. Brown, B. Zhang, B. Svirchuk, and M. Ni, "An experimental study of acoustic distributed beamforming using round-trip carrier synchronization," in *Proc. IEEE Int. Symp. Phased Array Syst. Technol. (ARRAY)*, Oct. 2010, pp. 316–323.
- [16] R. Preuss and D. R. Brown, III, "Retrodirective distributed transmit beamforming with two-way source synchronization," in *Proc. Conf. Inf. Sci. Syst. (CISS)*, Princeton, NJ, USA, Mar. 2010, pp. 1–6.
- [17] R. Preuss and D. R. Brown, III, "Two-way synchronization for coordinated multi-cell retrodirective downlink beamforming," *IEEE Trans. Signal Process.*, vol. 59, no. 11, pp. 5415–5427, Nov. 2011.
- [18] R. Mudumbai, D. R. Brown, III, U. Madhow, and H. V. Poor, "Distributed transmit beamforming: challenges and recent progress," *IEEE Commun. Mag.*, vol. 47, no. 2, pp. 102–110, Feb. 2009.
- [19] G. Giorgi and C. Narduzzi, "Performance analysis of Kalman-filter-based clock synchronization in IEEE 1588 networks," *IEEE Trans. Instrum. Meas.*, vol. 60, no. 8, pp. 2902–2909, 2011.
- [20] H. Kim, X. Ma, and B. R. Hamilton, "Tracking low-precision clocks with time-varying drifts using Kalman filtering," *IEEE/ACM Trans. Netw.*, vol. 20, no. 1, pp. 257–270, 2012.
- [21] A. Bletsas, "Evaluation of Kalman filtering for network time keeping," *IEEE Trans. Ultrason., Ferroelectr., Freq. Control*, vol. 52, no. 9, pp. 1452–1460, Sep. 2005.
- [22] L. Auler and R. d'Amore, "Adaptive Kalman filter for time synchronization over packet-switched networks: An heuristic approach," in *Proc. 2nd Int. Conf. Commun. Syst. Softw. Middleware (COMSWARE)*, Jan. 2007, pp. 1–7.
- [23] K. R. Brown, Jr., "The theory of the GPS composite clock," in *Proc. 4th Int. Tech. Meet. Satell. Div. Inst. of Navigat. (ION GPS-91)*, 1991, vol. 1, pp. 223–241.
- [24] D. Mills, A. Thyagarajan, and B. Huffman, "Internet timekeeping around the globe," in *Proc. Precision Time Interval (PTTI) Appl. Plann. Meet.*, Dec. 1997, pp. 365–371.
- [25] H. Abubakari and S. Sastry, "IEEE 1588 style synchronization over wireless link," in *Proc. IEEE Int. Symp. Precision Clock Synchron. Meas., Control, Commun. (ISPCS)*, Sep. 2008, pp. 127–130.
- [26] A. Kumar, R. Mudumbai, S. Dasgupta, M. Rahman, D. Brown III, M. Madhow, and P. Bidigare, "A scalable feedback mechanism for distributed nullforming with phase-only adaptation," *IEEE Trans. Signal Process.*, submitted for publication.
- [27] J. Hoydis, S. ten Brink, and M. Debbah, "Massive MIMO: How many antennas do we need?," in *Proc. 49th Annu. Allerton Conf. Commun., Control, Comput. (Allerton)*, 2011, pp. 545–550.
- [28] E. Larsson, O. Edfors, F. Tufvesson, and T. Marzetta, "Massive MIMO for next generation wireless systems," *IEEE Commun. Mag.*, vol. 52, no. 2, pp. 186–195, Feb. 2013.
- [29] C. Kominakis, C. Fragouli, A. Sayed, and R. Wesel, "Multi-input multi-output fading channel tracking and equalization using Kalman estimation," *IEEE Trans. Signal Process.*, vol. 50, no. 5, pp. 1065–1076, May 2002.
- [30] L. Galleani, "A tutorial on the 2-state model of the atomic clock noise," *Metrologia*, vol. 45, no. 6, pp. S175–S182, Dec. 2008.

- [31] G. Giorgi and C. Narduzzi, "Performance analysis of Kalman filter-based clock synchronization in IEEE 1588 networks," in *Proc. Int. IEEE Symp. Precision Clock Synchron. Meas., Control, Commun.*, Oct. 12–16, 2009, pp. 1–6.
- [32] Rakon RFPO45 SMD oven controlled crystal oscillator datasheet, 2009 [Online]. Available: <http://www.rakon.com/products/families/download/file?fid=39.133>
- [33] W. Klepczynski and P. Ward, "Frequency stability requirements for narrow band receivers," in *Proc. 32nd Annu. Precise Time/Time Interval Meet.*, Vienna, VA, USA, Nov. 2000.
- [34] D. Rife and R. Boorstyn, "Single-tone parameter estimation from discrete-time observations," *IEEE Trans. Inf. Theory*, vol. 20, no. 5, pp. 591–598, Sep. 1974.
- [35] Y. Bar-Shalom, X. R. Li, and T. Kirubarajan, *Estimation With Applications to Tracking And Navigation*. New York, NY, USA: Wiley, 2001.
- [36] B. Anderson and J. Moore, *Optimal Filtering*. New York, NY, USA: Dover, 1979.
- [37] B. Anderson, "Stability properties of Kalman-Bucy filters," *J. Franklin Inst.*, vol. 291, no. 2, pp. 137–144, 1971.
- [38] G. Lachapelle, M. Cannon, and G. Lu, "High-precision GPS navigation with emphasis on carrier-phase ambiguity resolution," *Marine Geodesy*, vol. 15, no. 4, pp. 253–269, 1992.
- [39] P. Smaragdis and P. Boufounos, "Learning source trajectories using wrapped-phase hidden Markov models," in *IEEE Workshop Appl. Signal Process. Audio Acoust.*, 2005, pp. 114–117.
- [40] K. Kastella, R. Mudumbai, and T. Stevens, "Frequency estimation in the presence of cycle slips: Filter banks and error bounds for phase unwrapping," in *Proc. IEEE Statist. Signal Process. Workshop (SSP)*, Aug. 2012, pp. 277–280.
- [41] J. Traa and P. Smaragdis, "A wrapped Kalman filter for azimuthal speaker tracking," *IEEE Signal Process. Lett.*, vol. 20, no. 12, pp. 1257–1260, Dec. 2013.
- [42] S. W. Chan, G. Goodwin, and K. S. Sin, "Convergence properties of the Riccati difference equation in optimal filtering of nonstabilizable systems," *IEEE Trans. Autom. Control*, vol. 29, no. 2, pp. 110–118, Feb. 1984.
- [43] C.-T. Chen, *Linear System Theory And Design*. London, U.K.: Oxford Univ. Press, 1999.
- [44] R. L. Williams, II and D. A. Lawrence, *Linear State-Space Control Systems*. New York, NY, USA: Wiley, 2007.



D. Richard Brown, III (S'97–M'00–SM'09) received the B.S. and M.S. degrees in Electrical Engineering from The University of Connecticut in 1992 and 1996, respectively, and received the Ph.D. degree in Electrical Engineering from Cornell University in 2000. From 1992–1997, he was with General Electric Electrical Distribution and Control. He joined the faculty at Worcester Polytechnic Institute (WPI) in Worcester, Massachusetts in 2000 and currently is an Associate Professor. He also held an appointment as a Visiting Associate Professor at

Princeton University from August 2007 to June 2008. His research interests are currently in coordinated wireless transmission and reception, synchronization, distributed computing, and game-theoretic analysis of communication networks.



Rui Wang (S'15) received the B.S. degree in Electrical Engineering from Nanjing University of Aeronautics and Astronautics (NUAA), China, in 2011. He received the M.S. degree in Electrical and Computer Engineering from Worcester Polytechnic Institute in 2013. He is currently a Ph.D. candidate at Worcester Polytechnic Institute. His research interests are currently in coordinated wireless transmission and reception, synchronization, and wireless power transfer.



Soura Dasgupta (M'87–SM'93–F'98) was born in 1959 in Calcutta, India. He received the B.E. degree in Electrical Engineering from the University of Queensland (Australia), in 1980, and the Ph.D. in Systems Engineering from the Australian National University in 1985. He is currently Professor of Electrical and Computer Engineering at the University of Iowa, U.S.A.

In 1981, he was a Junior Research Fellow in the Electronics and Communications Sciences Unit at the Indian Statistical Institute, Calcutta. He has held visiting appointments at the University of Notre Dame, University of Iowa, Université Catholique de Louvain-La-Neuve, Belgium and the Australian National University.

Between 1988 and 1991, 1998 to 2009 and 2004 and 2007 he respectively served as an Associate Editor of the IEEE TRANSACTIONS ON AUTOMATIC CONTROL, IEEE Control Systems Society Conference Editorial Board, and the IEEE TRANSACTIONS ON CIRCUITS AND SYSTEMS-II. He is a co-recipient of the Gullimen Cauer Award for the best paper published in the IEEE TRANSACTIONS ON CIRCUITS AND SYSTEMS in the calendar years of 1990 and 1991, a past Presidential Faculty Fellow, a subject editor for the *International Journal of Adaptive Control and Signal Processing*, and a member of the editorial board of the *EURASIP Journal of Wireless Communications*. In 2012 he was awarded the University Iowa Collegiate Teaching award. In the same year he was selected by the graduating class for an award on excellence in teaching and commitment to student success.

His research interests are in Controls, Signal Processing and Communications. He was elected as a Fellow of the IEEE in 1998.